RSC Advances

PAPER

Cite this: *RSC Adv.*, 2016, **6**, 104513

A DFT study on the interaction between 5-fluorouracil and $B_{12}N_{12}$ nanocluster

Masoud Bezi Javan,[a] Alireza Soltani,*[b] Zivar Azmoodeh,[c] Nafiseh Abdolahi[b] and Niloofar Gholami[d]

Received 17th July 2016
Accepted 22nd September 2016

DOI: 10.1039/c6ra18196a

www.rsc.org/advances

The electronic and optical properties of the 5-fluorouracil (5-FU) on $B_{12}N_{12}$ surface were investigated theoretically by pure and time-dependent density functional theory (TD-DFT) calculations. Herein, the $B_{12}N_{12}$ nanocluster is utilized as a drug delivery vehicle for both the free and tautomeric forms of 5-FU drug. Our study indicates that the adsorption energy of 5-FU is an exothermic process with negative values of a few hundreds up to −1.779 eV, depending on their interaction configurations. The results show that the 5-FU drug is covalently bonded to the surface of its nitrogen head, whereas the other forms represent weak interactions due to noncovalent bonds between two species. The tautomeric forms of 5-FU and the free forms of the adsorbate show different behavior of binding energies and the changes in molecular energy gaps.

1. Introduction

Nanotechnology has attracted much attention owing to its interesting applications in the medical field, such as medical devices and pharmaceutical studies.[1] The use of nanoscale devices and materials for diagnosis, treatment and drug delivery for chemotherapy have resulted in effective treatment with low side effects.[2,3] 5-Fluorouracil (5-FU) is a known anticancer drug, which can play an active role in the treatment of colon and breast cancers.[4,5] The structure of 5-FU is similar to that of uracil. 5-FU is one of the pyrimidine bases that are used as cytostatic agents in oncology. The significance of 5-FU in cancer chemotherapy and in diagnostics using ^{19}F MRI and MRS centralized spectroscopy have spanned vast experimental and clinical *in vitro* and *in vivo* reports.[6–12]

In the modern era of nanotechnology, massed nanomaterials have replaced bulk substrates in a vast range of applications because of their unprecedented properties. Out of the numerous inorganic nanomaterials, boron nitride (BN) and analogues of carbon nanocages have gained research attention because of their wider range of excellent properties such as high temperature and oxidation stability, low dielectric constant, high thermal conductivity and constant band gap with semiconductor nature than carbon. Recent studies on the structural properties and stability of the fullerene-like cages of $(BN)_n$ nanomaterials have indicated that the most stable nanocage is where $n = 12$, *i.e.*, $B_{12}N_{12}$, which consists of six tetragon rings and eight hexagon rings.[13–15] The interaction of adenine, uracil, and cytosine amino acids over BN and AlN nanocages were studied using DFT calculations.[16] The results reveal that the $B_{12}N_{12}$ nanocage has more sensitivity to these amino acids than $Al_{12}N_{12}$ nanocage. We have previously reported a DFT study of 5-FU adsorption onto a perfect and metal-doped BN nanotube in the gas phase by B3LYP functional.[17] We have shown that the adsorption of 5-FU as an anticancer drug over a pure substrate has an electrostatic nature. In addition, the drug molecule interacts with Ga-doped BN nanotubes and presents a strong interaction and high sensitivity to the presence of the drug, which was also compared to Al and Ge doping.

Several studies can be found that include extensive work on BN nanostructures. BN nanocages have large HOMO–LUMO gaps and lower interaction with the molecules.[14] There are several published papers on the gain of surface sensitivity with doping, particularly for hydrogen storage.[18,19] For instance, Wu *et al.* showed that the Li-doped $(BN)_xC_{1-x}$ structure can change the adsorption energy of H_2 molecules significantly.[18] Hu *et al.* showed that doping of the carbon atom enhances the hydrogen adsorption capacity of the BN nanocage.[19]

In 2015, Yaraghi *et al.* studied the adsorption of 5-fluorouracile tautomers on the surface of silicon graphene nanosheets using DFT calculations. They showed that the binding energy of the di-keto form is the most stable structure in comparison with keto–enol and di-enol forms.[20] Faria and Queiroz experimentally reported the interaction of TiO_2/ZnS nanotubes with 5-FU as an anticancer drug used in photodynamic therapy.[21]

The main purposes of the present investigation are to assess the electronic properties, charge transfer, and binding energy of

[a]*Physics Department, Faculty of Sciences, Golestan University, Gorgan, Iran*
[b]*Golestan Rheumatology Research Center, Golestan University of Medical Science, Gorgan, Iran. E-mail: Alireza.soltani46@yahoo.com; g.chem1983@gmail.com; Tel: +98-938-4544921*
[c]*Department of Physics, Payame Noor University, P. O. Box 19395-3697, Tehran, Iran*
[d]*Young Researchers and Elite Club, Gorgan Branch, Islamic Azad University, Gorgan, Iran*

5-FU drug molecule with $B_{12}N_{12}$ nanocage and to clarify both strong and weak modification of the drug molecule properties when located on the $B_{12}N_{12}$ nanocage.

2. Computational details

Theoretical calculations were performed using Perdew–Burke–Ernzerhof (PBE) functional[22] augmented with an empirical dispersion term (PBE-D) and then compared with B3LYP-D functional[23,24] and 6-311+G** basis set as implemented using the GAMESS suite of programs.[25] The PBE density functional has been previously reported to study BN nanostructures.[26–29] The GaussSum program has been applied to get the density of state plot (DOS).[30] Moreover, the corresponding optical adsorption spectra were obtained *via* time-dependent density functional theory (TD-DFT) computations (B3LYP/6-311+G**) in the gas phase regime.[31,32] Based on the natural bond orbitals (NBO), the charges on boron and nitrogen atoms in $B_{12}N_{12}$ nanocluster are 1.101 and −1.101 |e|, showing the strong ionic nature of the boron-nitrogen bonds. Spin multiplicity of the drug molecule was set to one with relevance to its molecular orbital of ground state (its ground electronic state is $^1\Sigma^+$). The optimized configurations were further subjected to harmonic vibrational frequency calculations at the PBE functional level. For all systems studied, the SCF convergence limit was set to 10^{-6} a.u. over energy and electron density. The basis set superposition error (BSSE) for the adsorption energy was corrected by implementing the counterpoise method.[33] Binding energies (E_b) were calculated using the following formula:

$$E_b = E_{complex} - (E_{nanocluster} + E_{5\text{-FU}}) + E_{BSSE} \quad (1)$$

where $E_{complex}$ is the total energy of the $B_{12}N_{12}$ interacting with the 5-FU molecule, $E_{nanocluster}$ is the total energy of the pure $B_{12}N_{12}$ nanocluster, and $E_{5\text{-FU}}$ is the total energy of an isolated 5-FU molecule.

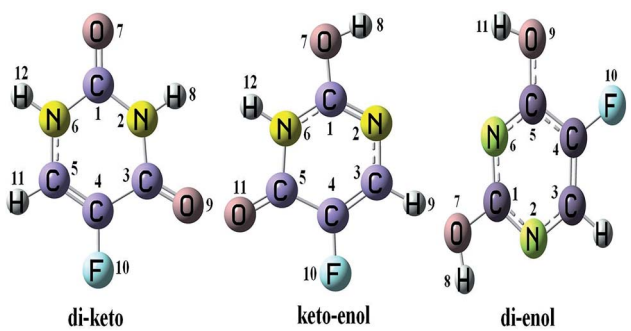

Fig. 1 Different structures of the 5-FU molecule.

3. Results and discussion

3.1 Structural analysis of 5-FU drug

The relaxed structural parameters of 5-FU drug as computed by PBE-D method in the gas phase are shown in Fig. 1 and summarized in Table 1. The calculated length of C4–F10 bond is 1.346 Å, by PBE-D method, which is in agreement with the experimental value of 1.348 Å.[34,35] Calculated bond lengths of C1–O7 (1.221 Å) and C3–N2 (1.417 Å) are also close to experimental results (C1–O7: 1.233 Å and C3–N2: 1.408 Å).[34,35] Therefore, we have found that the PBE-D method is more suitable (due to its closeness to the experimental data) than the B3LYP-D method to assess the accuracy of the geometry relaxations. We have observed that the charges of O7, O9, and F10 atoms by PBE-D functional are −0.316, −0.277, and −0.154 e, respectively, whereas both carbonyl oxygen atoms, O7 (−0.493 e) and O9 (−0.477 e), in 5-FU represent higher values of negative charge by B3LYP-D functional. The charge of the F atom by PBE-D is −0.154 e, whereas it increases to −0.277 e using B3LYP-D functional.

3.2 Structural analysis of 5-FU loaded onto $B_{12}N_{12}$

Fig. 2 presents the relaxed structure of $B_{12}N_{12}$ nanocage using DFT calculations using the PBE-D method. The effects of 5-FU adsorption on the $B_{12}N_{12}$ nanocage were investigated in four states, the original (di-keto) form and six tautomer states (keto–enol and di-enol), using DFT calculations, as well as PBE-D level of theory, chosen for accuracy of the geometry optimizations (see Fig. 3). The relaxed bond lengths and angles as obtained from the DFT calculations are in good agreement with the experimental data. The computed values of bond lengths associated with equilibrium formation of 5-FU adsorbed onto the $B_{12}N_{12}$ nanocage are summarized in Table 2.

As shown in Table 2, significant changes in the length of B–N bonds can be observed in A and K configurations. A decline in the binding energy is observed with increasing distance between the 5-FU molecule and the nanocage (Table 2). The distance of the 5-FU molecule to the nanocage is approximately large, indicating a physical adsorption-like bonding. Within the $B_{12}N_{12}$ nanocage, the average B–N distances are increased from 1.491 Å to 1.620 (A), 1.568 (B), 1552 (C), and 1.545 Å (D). The N–H distances after the adsorption processes are 1.082 (A), 1.022 (B), 1.023 (C), and 1.072 Å (D) in comparison with the pure 5-FU (1.01 Å). Other adsorption sites led to an evident difference in the geometric model, as shown in Table 1. In agreement with

Table 1 Optimized structural geometries of 5-FU using the PBE method. Lengths are in angstrom (Å)

Property	C1–N2	C1–N6	C1–O7	C3–O9	C4–F10	C5–N6	C3–C4	N6–H12	O7–H8
Di-keto	1.396	1.398	1.221	1.222	1.346	1.381	1.466	1.016	—
keto–enol	1.306	1.361	1.347	1.223	1.347	1.427	1.367	1.021	0.977
Di-enol	1.340	1.341	1.350	1.344	1.352	1.332	1.385	—	0.976

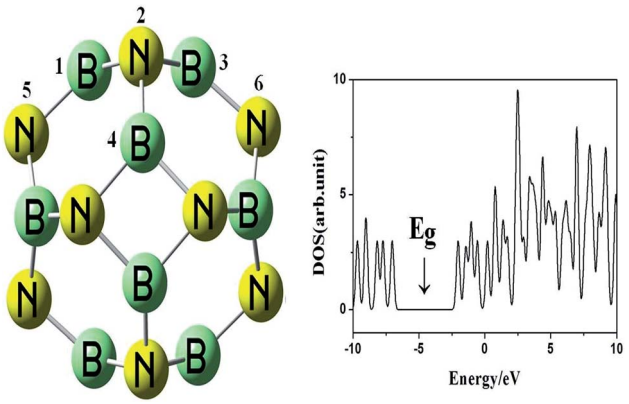

Fig. 2 The optimized $B_{12}N_{12}$ nanocage and its DOS plot.

previous reports,[18] we found that the binding of 5-FU in tautomer forms compared to the original form are the more energetically favorable and the difference in energy of these configurations would be large. The computed binding energies in the A, B, C, and D forms are −0.0453, −0.0267, −0.0310, and −0.0399 eV, respectively, representing the binding of 5-FU over $B_{12}N_{12}$ that comes from the hybridization of the O-2p and N-2p orbitals with the B-2p orbitals, whereas the adsorption of 5-FU (original form) interacting with $B_{12}N_{12}$ nanocage can be attributed to the electrostatic bond in the interaction process (see Fig. 3).[36] In Fig. 4, we have shown the charge density distribution around interacting atoms of the 5-FU and BN nanocage from A to K configurations. The contour plot of charge density in the interacting regions of the 5-FU molecules with $B_{12}N_{12}$ nanoclusters can show the strength of the orbital hybridization for all examined configurations due to changes in the nature of the atomic orbital charge distribution of the adsorbent and host nanocage. In many cases, deviation from spherical symmetry around interacting molecules is not very high, which implies the electrostatic nature of the interaction. However, the charge density distributions of F, G and K states show high density and non-covalent bonding between 5-FU molecule and $B_{12}N_{12}$ nanocluster, as presented in Table 2.

Table 3 presents the values of Gibbs free energies (ΔG), enthalpy changes (ΔH), and entropic changes (ΔS) in all examined configurations. The values of ΔG, ΔH, and ΔS for the forms A, B, C, and D are negative. The lowering of ΔG proves the weakening of the 5-FU adsorption onto the $B_{12}N_{12}$ nanocage.[15] The computed ΔG values in E, F, G, K, and J forms are −12.279, −44.304, −30.489, −16.498, and −38.477 kcal mol^{-1}, whereas

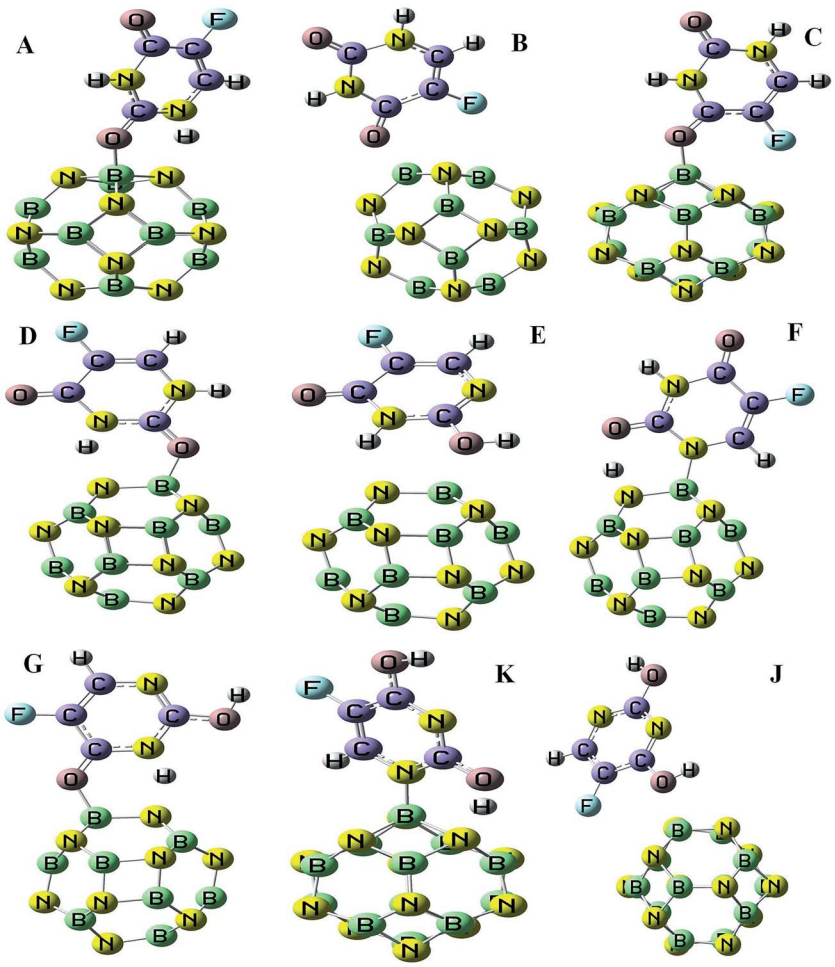

Fig. 3 Relaxed structures of nine stable configurations for the adsorption states of 5-FU onto the pure $B_{12}N_{12}$ nanocage.

Table 2 The structural and electronic parameters of 5-FU molecule over $B_{12}N_{12}$ nanocage

Property	Pure	A	B	C	D	E	F	G	J	K
B–N/Å	1.491	1.620	1.568	1.552	1.545	1.521	1.574	1.559	1.523	1.607
N–H/Å	—	1.082	1.022	1.023	1.072	1.039	1.021	1.121	—	—
C–O/Å	—	1.277	1.261	1.259	1.274	1.220	1.221	1.282	1.374	1.305
O–H/Å	—	—	—	—	—	0.981	1.540	0.977	0.983	1.058
N–B–N/°	126.03	115.85	117.42	117.87	116.29	121.81	113.59	115.33	95.78	91.06
E_{HOMO}/eV	−7.03	−6.4	−5.98	−5.92	−6.2	−6.22	−6.29	−6.17	−6.62	−6.49
E_{LUMO}/eV	−2.04	−3.53	−4.22	−4.22	−3.48	−2.60	−2.67	−3.46	−2.98	−3.43
E_g/eV	4.99	2.87	1.79	1.70	2.72	3.62	3.62	2.71	3.64	3.06
ΔE_g/eV	—	−42.49	−64.13	−65.93	−45.49	−27.45	−27.45	−45.69	−27.05	−38.68
E_{ad}/eV	—	−0.045	−0.027	−0.031	−0.040	−0.753	−1.779	−1.319	−0.480	−1.525
E_{BSSE}/eV	—	−0.031	−0.016	−0.022	−0.029	−0.623	−1.486	−1.114	−0.370	−1.245
D/Å	—	1.573	1.636	1.626	1.590	1.853	1.563	1.558	1.943	1.607
DM/Debye	0.0	3.978	11.395	11.546	8.785	3.778	4.319	7.958	4.210	4.773
E_F/eV	−4.535	−4.965	−5.10	−5.07	−4.48	−4.41	−4.48	−4.82	−4.80	−4.96

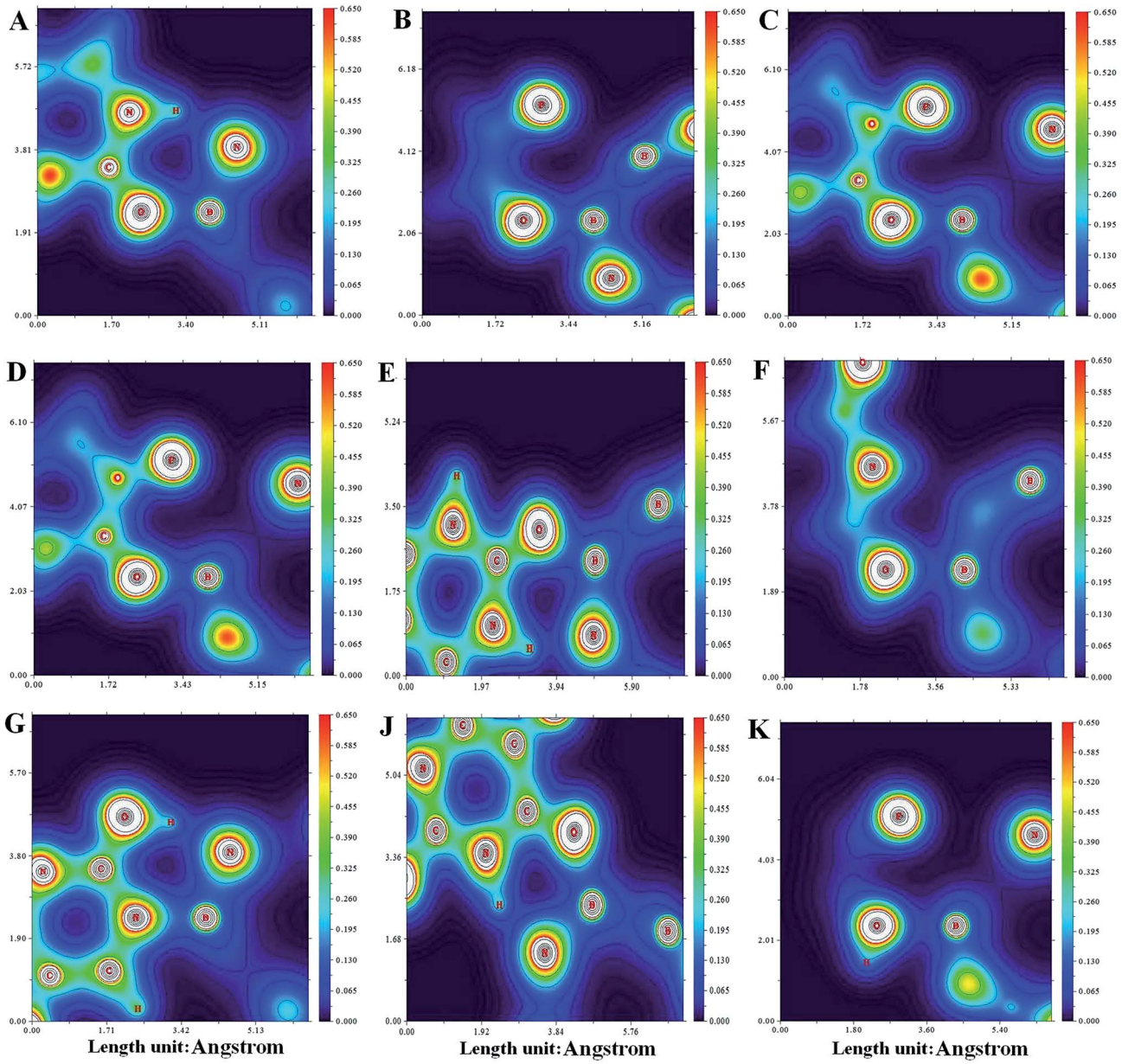

Fig. 4 Contour plots of charge density for 5-FU drug adsorbed on $B_{12}N_{12}$ nanocluster.

Table 3 The values of Gibbs free energy (ΔG), enthalpy change (ΔH), and entropic change (ΔS) in all examined configurations

Property	H	E	E_0	G	S	ΔS	ΔE_0	ΔH	ΔG	CV	ZPE
5-FU	−513.57	−513.57	−513.58	−513.61	83.87	—	—	—	—	27.29	47.74
$B_{12}N_{12}$	−955.03	−955.03	−955.05	−955.05	98.62	—	—	—	—	53.82	78.21
A	−1468.638	−1468.639	−1468.658	−1468.705	141.64	−41.68	−17.583	−23.862	−28.258	85.60	126.45
B	−1468.689	−1468.623	−1468.643	−1468.689	141.57	−41.75	−8.163	−55.888	−18.211	86.19	127.03
C	−1468.625	−1468.626	−1468.645	−1468.689	133.94	−49.38	−9.419	−15.699	−18.211	84.07	127.17
D	−1468.643	−1468.644	−1468.663	−1468.709	140.15	−43.17	−20.722	−27.002	−30.770	85.32	126.36
E	−1468.601	−1468.602	−1468.621	−1468.669	143.34	−39.98	−6.570	−7.163	−12.279	86.34	126.24
F	−1468.654	−1468.655	−1468.674	−1468.720	139.23	−44.09	−39.851	−40.445	−44.304	85.29	126.32
G	−1468.631	−1468.632	−1468.651	−1468.698	140.17	−43.15	−25.409	−26.001	−30.489	85.48	125.52
J	−1468.592	−1468.593	−1468.612	−1468.670	140.15	−43.17	−0.918	−4.952	−16.498	85.52	126.39
K	−1468.640	−1468.641	−1468.660	−1468.705	137.02	−46.30	−35.094	−35.095	−38.477	84.73	126.50

the ΔH values are −7.163, −40.445, −26.001, −4.952, and −35.095 kcal mol^{-1}, respectively. The thermodynamic parameters imply that the adsorption of 5-FU in keto–enol form (F) is strongly favorable as the drug can be adsorbed spontaneously on the surface of an adsorbent.

The significance of the bond reorganization energy (E_{br}) of the deformation degree in the geometry of $B_{12}N_{12}$ nanocluster for the adsorption of 5-FU molecule was calculated. The values of E_{br} for $B_{12}N_{12}$ interacting with 5-FU in the forms A, B, C, and D are found to be 0.728, 0.580, 0.564, and 0.819 eV, respectively, suggesting a weak physical bond between the nanocage and the molecule. In comparison with carbonyl and hydroxyl models, the 5-FU tautomer from its nitrogen head has better adsorption energy over the surface of the $B_{12}N_{12}$ nanocage. As listed in Table 1, the order for the adsorption energy in tautomer forms is F > K > G > E > J. As shown in Table 1, significant changes in the bond length and bond angle were also observed. The interaction distances for the five adsorption forms ranged from 1.558 to 1.943 Å. The adsorption of 5-FU onto the nanocage increases the B–N distance from 1.491 Å in the free form to 1.521 (E), 1.574 (F), 1.559 (G), 1.523 (J), and 1.607 Å (K). In contrast, the adsorption energy of 5-FU drug in tautomer forms, di-enol form (J: −0.480 eV) is very weak compared to the keto–enol form (F: −1.779 eV), which is stronger than silicon graphene nanosheet and boron nitride nanotube.[18] We also found that the values of E_{br} in E, F, G, K, and J forms are 0.204, 1.28, 0.871, 0.847, and 0.146 eV, respectively, indicating a strong chemical bond in the keto–enol form (F) compared to di-enol form (K). Electronegative atoms such as N atom of the drug molecule, with a negative charge of about −0.209 |e|, affect a different degree of charge distribution between both atoms of the drug (0.143 |e|) and the nanocluster (1.101 |e|) when directly interacting with the B atom of the $B_{12}N_{12}$, which carries a positive atomic charge of about 0.119 |e|. In this interaction, the electron pair belonging to N atom of the adsorbate in a covalent bond was donated and shared with the B atom of the adsorbent, indicating a strong chemical bond between both structures. In the most stable configurations (F and K systems) it has been found that the charges of about 0.763 and 0.198 |e| are transferred from the nanocluster to the drug molecule by NBO analysis, which indicates that the nanocage functions as an electron donor and the drug molecule functions as an electron acceptor.

The density of states (DOS) of the $B_{12}N_{12}$/5-FU complex in different forms has been compared to the pure $B_{12}N_{12}$ nanocluster and 5-FU molecule. It can be clearly seen in Fig. 5 that the DOS of $B_{12}N_{12}$ is affected considerably due to the interaction with the 5-FU molecule. Of all the forms considered in the interaction, form C has the most significant change on HOMO–LUMO gap with an amount of 1.70 eV, whereas the HOMO–LUMO gap of $B_{12}N_{12}$ nanocluster is 4.99 eV. In accordance with the DOS plot results presented in Table 1, HOMO–LUMO energy gap decreases in the B and C forms with increasing Fermi energy levels; both forms have slight variations in the value of −5.10 and −5.07 eV, respectively. Hazrati *et al.* showed that the 5-FU molecule can be physically adsorbed on C_{60} fullerene.[36] They have used different DFT functional to investigate the electronic structure of the 5FU–C_{60} complex and generally found that the HOMO–LUMO gap of the C_{60} fullerene is slightly smaller due to the adsorption of 5-FU.

We have calculated the energies of both HOMO (highest occupied molecular orbital) and LUMO (lowest unoccupied molecular orbital) orbitals using PBE functional and 6-311++G** basis set in different positions of the drug molecule. The HOMO energy values in forms A, B, C, and D are altered to −6.40, −5.98, −5.92, and −6.20 eV, whereas this value for the adsorbent is −7.03 eV. In contrast, the LUMO energy values for the same forms are −3.53, −4.22, −4.22, −3.48 eV, whereas for the pure adsorbent the value is −2.04 eV. Moreover, there are considerable changes in the LUMO values for the mentioned configurations when compared with the pure adsorbent. In forms B and C, the LUMO energy is more affected with a variation of about 2.18 eV. In Fig. 6, the HOMO, HOMO−4, HOMO−10, HOMO−16 and LUMO, LUMO+4, LUMO+10, LUMO+16 wave functions are shown for the F configuration, as the most affected states of the stable 5-Fu->BN adsorbed system. It is known that the wave function distributions show the active sites of the molecule and it is important for protection of the drug activity during interaction with the nanocage as a drug carrier. It can be clearly observed that more than 90% of the wave function is distributed on the 5-FU molecule, implying that the activity of the drug is owing to the interaction with $B_{12}N_{12}$ nanocluster.

The infrared (IR) spectrum of 5-FU molecule was recorded in the 3600–400 cm^{-1} spectral region in the different states, as shown in Fig. 7. The strongest peaks at 1625 and 1787 cm^{-1} (A),

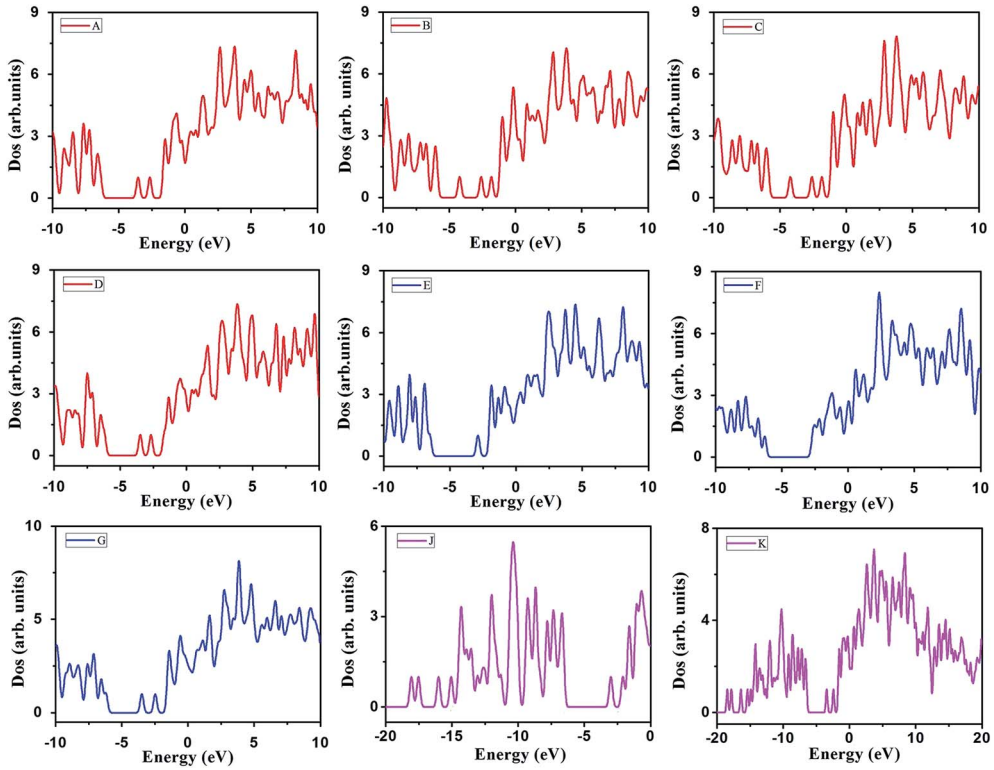

Fig. 5 Calculated DOS plots of 5-FU drug adsorbed over $B_{12}N_{12}$ nanoclusters at the different states.

1616 and 1786 cm^{-1} (B), 1665 and 1750 cm^{-1} (C), and 1669 and 1738 cm^{-1} (D) are assigned to the C3═O9 and C1═O7 groups of 5-FU/$B_{12}N_{12}$ complex, whereas the bonds of maximum intensity at 1725 and 1759 cm^{-1} are assigned to the C3═O9 and C1═O7 groups in the free 5-FU molecule, respectively. The IR spectrum indicates significant changes in the C4–F10 stretching

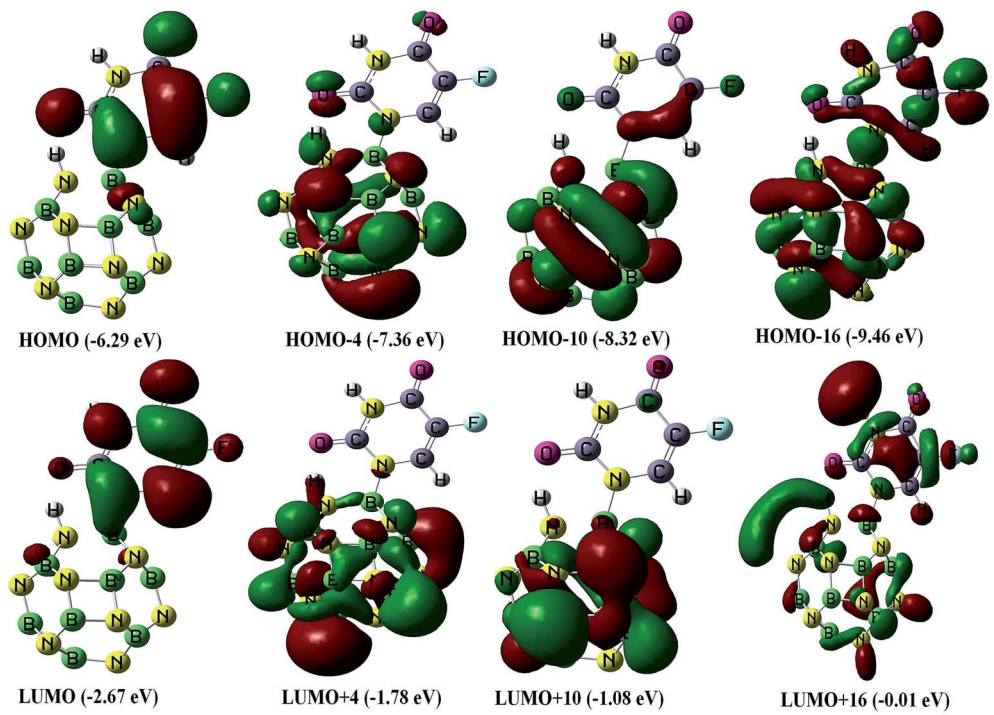

Fig. 6 The HOMO and LUMO orbitals of the 5-FU molecule adsorbed on $B_{12}N_{12}$ nanocluster in F configuration.

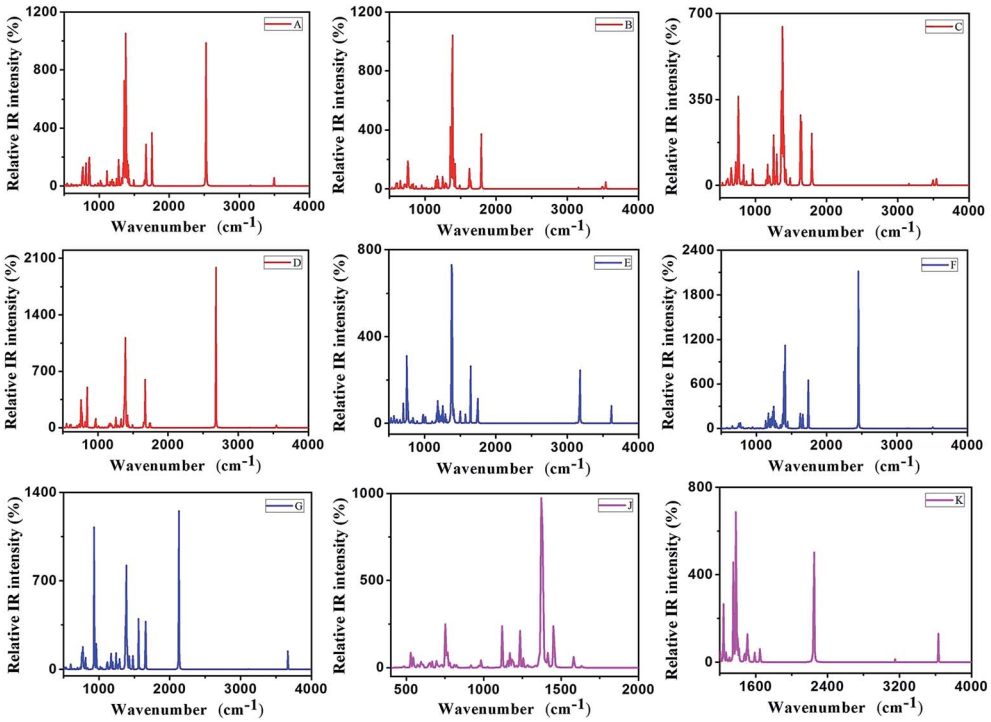

Fig. 7 IR spectrum of 5-FU drug adsorbed over $B_{12}N_{12}$ nanocages at the different states.

Table 4 Selected excitation energies (*E*, nm), oscillator strength (*f*), Wavelength (λ_{max}/nm), and relative orbital contributions calculated by B3LYP functional

Structure	Energy/eV	Wavelength/nm	*f*	Assignment
$B_{12}N_{12}$	0.612	506.27	0.0001	H−2 → L+1 (−24%), H−1 → L (38%), H → L+1 (−13%)
	0.637	486.26	0.0001	H → L (32%), H → L+2 (20%)
	0.699	443.16	0.0001	H−2 → L+2 (42%), H → L+1 (21%)
A	4.031	307.54	0.0009	H → L (99%)
	4.234	292.79	0.0008	H−2 → L (24%), H−1 → L (73%)
	4.334	286.04	0.0001	H−2 → L (73%), H−1 → L (−26%)
B	2.712	457.09	0.0049	H−1 → L (−34%), H → L (63%)
	2.807	441.61	0.0218	H−1 → L (63%), H → L (36%)
	3.054	405.98	0.0007	H−2 → L (99%)
C	2.675	463.50	0.0001	H → L (98%)
	2.814	440.49	0.0001	H−1 → L (96%)
	3.037	408.25	0.0007	H−2 → L (99%)
D	3.865	320.74	0.0005	H → L (99%)
	4.179	296.68	0.0001	H−2 → L (22%), H−1 → L+1 (74%)
	4.225	293.40	0.0001	H−2 → L (70%), H−1 → L (−25%)
E	4.749	261.05	0.1010	H−4 → L (−26%), H → L (64%)
	4.761	260.37	0.0494	H−4 → L (52%), H → L (31%)
	5.179	239.38	0.0004	H−1 → L (97%)
F	4.764	260.25	0.0001	H−2 → L (90%)
	4.823	257.05	0.2565	H → L (93%)
	4.949	250.48	0.0001	H → L+1 (99%)
G	3.715	333.70	0.0044	H → L (99%)
	4.154	298.42	0.0001	H−1 → L (89%)
	4.224	293.52	0.0001	H−2 → L (82%), H−1 → L (−10%)
J	4.73	262.16	0.0817	H → L (94%), H−1 → L (2%)
	4.82	257.10	0.0057	H−7 → L (83%), H−6 → L (6%), H−4 → L (6%)
	4.83	256.94	0.0035	H−1 → L (93%), H−7 → L (2%), H → L (2%)
K	4.09	303.12	0.0003	H → L (98%)
	4.29	288.69	0.0008	H−2 → L (26%), H−1 → L (69%), H−5 → L (2%)
	4.43	278.54	0.0006	H−2 → L (71%), H−1 → L (28%)
	4.43	278.54	0.0006	H−2 → L (71%), H−1 → L (28%)

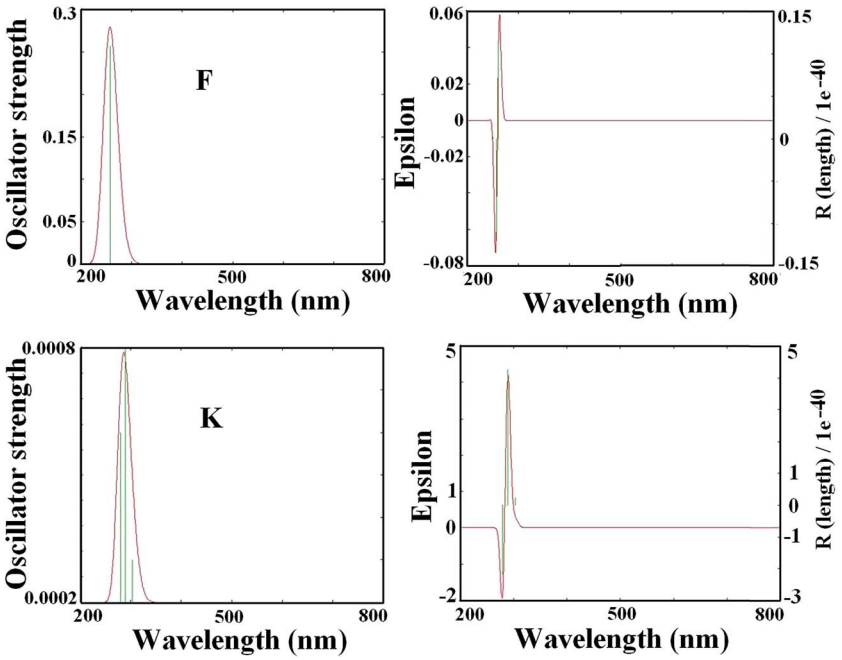

Fig. 8 The optical absorption spectra of 5-FU–$B_{12}N_{12}$ nanoclusters in F and K configurations.

bonds appearing at 1250 (A), 1247 (B), 1251 (C), and 1248 cm^{-1} (D) in comparison with the isolated state (1227 cm^{-1}), which is in excellent agreement with the results reported by Pavel and co-workers.[37]

Experimental vibrational frequency of the 5-FU molecule was previously studied by Rastogi and Palafox.[38] They reported that the 5-FU molecule has intensive peaks at frequency intervals between 400 and 3000 cm^{-1}, which is in agreement with our results.[39] In its monomer form, peaks of the CN_3–H, C–F, C4=O, C_2=O, N_3–H and N_1–H bonds of 5-FU appear at 758, 1254, 1748, 1764, 3491, and 3510 cm^{-1}, respectively. Our results also present an increase in bond length of C=O, C–C and N–H bonds agreeing combined mode's change to lower frequencies and increase in bond strength with an adsorbent surface and simultaneous decrement in bond length of C–F and C–H bonds agreeing recognized mode's changes to higher frequencies. After the interaction between 5-FU and $B_{12}N_{12}$ nanocage, the C4–C5 bonding frequency mode of the adsorbed molecule appears at lower values and is slightly altered from 1652 cm^{-1} to 1651 (A), 1641 (B), 1636 (C), 1638 cm^{-1} (D) compared with a value of 1671 cm^{-1} (5-FU molecule) recently reported by Simonetti[40] and Rastogi.[41] The IR spectrum of the free 5-FU exhibits a decrease in bond strength for the ring N–H wagging mode at about 1451 cm^{-1},[42] which, upon interaction with adsorbent, decreases to 1430 (A), 1418 (B), 1421 (C), and 1425 cm^{-1} (D).

For further investigation the optical properties of 5-FU interacting with $B_{12}N_{12}$ nanocluster was provided by TDDFT-(B3LYP/6-311+G**) calculations in gas phase.[43] Shown in Table 4, the excitation energies and oscillator strengths of all states of the adsorbing 5-FU complexes in free and tautomeric forms were calculated and studied. The structure of $B_{12}N_{12}$ has one considerable peak with the energy of 5.844 eV and an adsorption wavelength of 212.13 nm. After adsorption of free form of 5-FU molecule in its most stable state, B, a significant peak is observed with energy of 2.807 eV and red-shifted wavelength of 441.61 nm. This is in contrast to $B_{12}N_{12}$ nanocage, which undergoes a hypsochromic or blue shift in the gas phase. The most important contribution observed in form B was from H−1 → L with 63% of the 0.0218 oscillator strength, mainly including the C3–O9 carbonyl group. There are contributions from three transitions for 5-FU adsorbed in tautomeric form, F, with the most important existence being H → L with 93% of the 0.2565 oscillator strength, which is predicted to be blue-shifted in this form (see Fig. 8). The results indicate that the adsorption intensity in F form is decreased from 5.83 to 4.823 eV owing to hypochromic effects. Furthermore, it is significant that, when 5-FU in form of tautomeric (F) is adsorbed over the $B_{12}N_{12}$ nanocage, the adsorption wavelength is significantly reduced to 257 nm, arising from H–L π/π^* transition.[44,45]

4. Conclusion

In conclusion, based on DFT and TD-DFT calculations, we have found that the electronic and optical properties of $B_{12}N_{12}$ nanocluster interacting with 5-FU molecule depend strongly on the binding nature of the interacting systems. Our study indicates that the adsorption energy of 5-FU in the exothermic process is negative, with values of a few hundreds up to −1.779 eV. The results show that the 5-FU drug towards its nitrogen head was covalently bonded to the surface of the substrate, whereas the other forms represent weak interactions due to noncovalent bonds between two species. The tautomeric forms of 5-FU and the free forms of adsorbate show the different behavior of binding energies and the changes in molecular energy gap. The obtained results for the 5-FU:$B_{12}N_{12}$ complex

demonstrate that the binding energy of the keto–enol form is more stable than both the di-keto and di-enol forms. The formation of covalent bonds between the carbonyl group of the 5-FU molecule and the boron atom of the substrate, accompanied by a charge transfer from the 5-FU to the nanocluster, resulted in E_g reduction and raising the electrophilicity and chemical potential of the substrate. Optical and vibrational frequency modes were studied for experimental confirmation of the considered systems.

Acknowledgements

We thank the clinical Research Development Unit (CRDU), Sayad Shirazi Hospital, Golestan University of Medical Sciences, Gorgan, Iran.

References

1 P. M. Tiwari, K. Vig, V. A. Dennis and R. Shree, *Nanomaterials*, 2011, **1**, 31.
2 K. Seino and W. G. Schmidt, *Surf. Sci.*, 2004, **548**, 183.
3 E. Duverger, T. Gharbi, E. Delabrousse and F. Picaud, *Phys. Chem. Chem. Phys.*, 2014, **16**, 18425.
4 C. H. Wu, C. Chen Wu and Y. S. Ho, *J. Cancer Mol.*, 2007, **3**, 15.
5 B. Ardalan, R. Luis, M. Jaime and D. Franceschi, *Cancer Invest.*, 1998, **16**, 237.
6 D. J. Brown, *Interscience*, New York, 1994.
7 A. F. Pozharskii, A. T. Soldatenkov and A. R. Katrizky, *Advanced synthesis and catalysis*, New York, 1997.
8 D. D. Berker, J. M. McGregor and B. R. Hughes, *Br. J. Dermatol.*, 2007, **156**, 222.
9 R. Freelove and A. D. Walling, *Am. Fam. Physician*, 2006, **73**, 485.
10 J. A. Saonere, *J. Pharm. Pharmacol.*, 2010, **4**, 314.
11 E. J. Choi and G. H. Kim, *Oncol. Rep.*, 2009, **22**, 1533.
12 B. Blicharskaa and T. Kupka, *J. Mol. Struct.*, 2002, **613**, 153.
13 X. F. Fan, Z. Zhu, Z. X. Shen and J.-L. Kuo, *J. Phys. Chem. C*, 2008, **112**, 15691.
14 A. J. Karttunen, M. Linnolahti and T. A. Pakkanen, *J. Phys. Chem. C*, 2008, **112**, 10032.
15 M. T. Baei, A. S. Ghasemi, E. Tazikeh Lemeski, A. Soltani and N. Gholami, *J. Cluster Sci.*, 2016, **1081**, 27.
16 M. T. Baei, M. R. Taghartapeh, E. T. Lemeski and A. Soltani, *Phys. B*, 2014, **444**, 6.
17 A. Soltani, M. T. Baei, E. Tazikeh Lemeski, S. Kaveh and H. Balakheyli, *J. Phys. Chem. Solids*, 2015, **86**, 57.
18 H. Y. Wu, X. F. Fan, J. L. Kuo and W. Q. Deng, *Chem. Commun.*, 2010, **46**(6), 883.
19 Z. Y. Hu, X. Shao, D. Wang, L. M. Liu and J. K. Johnson, *J. Chem. Phys.*, 2014, **141**(8), 084711.
20 A. Yaraghi, O. M. Ozkendir and M. Mirzaei, *Superlattices Microstruct.*, 2015, **85**, 784.
21 H. A. Mendonça Faria and A. A. Alencar de Queiroz, *Mater. Sci. Eng., C*, 2015, **56**, 260.
22 J. P. Perdew, K. Burke and M. Ernzerhof, *Phys. Rev. Lett.*, 1996, **77**, 3865.
23 A. D. Becke, *J. Chem. Phys.*, 1993, **98**, 5648.
24 T. C. Lee, W. T. Yang and R. G. Parr, *Phys. Rev. B: Condens. Matter Mater. Phys.*, 1988, **37**, 785.
25 M. W. Schmidt, K. K. Baldridge, J. A. Boatz, S. T. Elbert, M. S. Gordon, J. H. Jensen, S. Koseki and N. Matsunaga, *J. Comput. Chem.*, 1993, **11**, 1347.
26 J. M. Matxain, L. A. Eriksson, J. M. Mercero, X. Lopez, M. Piris, J. M. Ugalde, J. Poater, E. Matito and M. Sola, *J. Phys. Chem. C*, 2007, **111**, 13354.
27 E. Duverger, T. Gharbi, E. Delabrousse and F. Picaud, *Phys. Chem. Chem. Phys.*, 2014, **16**, 18425.
28 E. M. Kumar, S. Sinthika and R. Thapa, *J. Mater. Chem. A*, 2015, **3**, 304.
29 Y. Guo and W. Guo, *J. Phys. Chem. C*, 2015, **119**, 873.
30 N. M. O'Boyle, A. L. Tenderholt and K. M. Langner, *J. Comput. Chem.*, 2008, **29**, 839.
31 F. D. Angelis and L. Armelao, *Phys. Chem. Chem. Phys.*, 2011, **13**, 467.
32 Y. Cui, Z. Lou, X. Wang, S. Yu and M. Yang, *Phys. Chem. Chem. Phys.*, 2015, **17**, 9222.
33 F. Tournus and J. C. Charlier, *Phys. Rev. B*, 2005, **71**, 165421.
34 B. Blicharska and T. Kupka, *J. Mol. Struct.*, 2002, **613**, 153.
35 G. Ferenczy, L. Harsanyi, B. Rozsondai and I. Hargittai, *J. Mol. Struct.*, 1986, **71**, 140.
36 M. Khodam Hazrati and N. L. Hadipour, *Phys. Lett. A*, 2016, **380**, 937.
37 I. Pavel, S. Cota, S. Cınta-Pınzaru and W. Kiefer, *J. Phys. Chem. A*, 2005, **109**, 9945.
38 V. K. Rastogi and M. A. Palafox, *Spectrochim. Acta, Part A*, 2011, **79**, 970.
39 D. P. Chong, *J. Chin. Chem. Soc.*, 2016, **63**(1), 109.
40 S. Simonetti, A. Dıaz Company, E. Pronsato, A. Juan, G. Brizuela and A. Lam, *Appl. Surf. Sci.*, 2015, **359**, 474.
41 V. K. Rastogi, V. Jain, R. A. Yadav, C. Singh and M. A. Palafox, *J. Raman Spectrosc.*, 2000, **31**, 595.
42 S. Farquharson, A. Gift, C. Shende, F. Inscore, B. Ordway, C. Farquharson and J. Murren, *Molecules*, 2008, **13**, 2608.
43 A. Soltani and M. Bezi Javan, *RSC Adv.*, 2015, **5**, 90621.
44 A. Soltani, A. Sousaraei, M. Bezi Javan, M. Eskandari and H. Balakheyli, *New J. Chem.*, 2016, **40**, 7018.
45 T. Gustavsson, A. Banyasz, E. Lazzarotto, D. Markovitsi, G. Scalmani, M. J. Frisch, V. Barone and R. Improta, *J. Am. Chem. Soc.*, 2006, **128**, 607.